

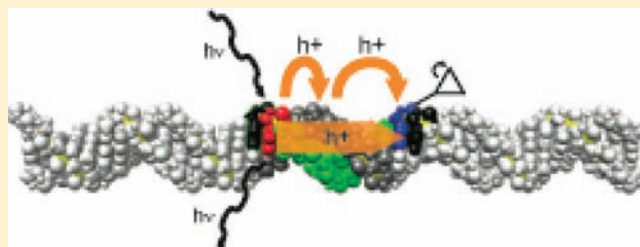
Single-Step Charge Transport through DNA over Long Distances

Joseph C. Genereux, Stephanie M. Wuerth, and Jacqueline K. Barton*

Division of Chemistry and Chemical Engineering, California Institute of Technology, Pasadena, California 91125, United States

S Supporting Information

ABSTRACT: Quantum yields for charge transport across adenine tracts of increasing length have been measured by monitoring hole transport in synthetic oligonucleotides between photoexcited 2-aminopurine, a fluorescent analogue of adenine, and N₂-cyclopropyl guanine. Using fluorescence quenching, a measure of hole injection, and hole trapping by the cyclopropyl guanine derivative, we separate the individual contributions of single- and multistep channels to DNA charge transport and find that with 7 or 8 intervening adenines the charge transport is a coherent, single-step process. Moreover, a transition occurs from multistep to single-step charge transport with increasing donor/acceptor separation, opposite to that generally observed in molecular wires. These results establish that coherent transport through DNA occurs preferentially across 10 base pairs, favored by delocalization over a full turn of the helix.



INTRODUCTION

The exceptional ability of DNA to mediate charge transport (CT) is the basis of novel molecular devices and may be exploited by the cell for both redox sensing and signaling.¹ The conduction properties of different DNA assemblies are found to be highly sensitive not only as to how the DNA is coupled within a particular assay but also as to how the DNA base pairs are dynamically stacked.² As a consequence, the sequence-dependent yields of DNA-mediated CT are not readily rationalized with superexchange and hopping through static structures.^{2,3}

DNA CT is mediated by the π -stack of the base pairs and, for well-coupled donors and acceptors, can lead to charge migration over 200 Å.^{2–4} For the quenching of photoexcited 2-aminopurine (Ap) by guanine across an adenine tract, the distance dependence is shallow but periodic with respect to tract length; the periodicity has been assigned as a consequence of transient delocalization over 4 A–T base pairs being ideal for forming a CT-active state.⁵ Evidence for delocalization has been found from other experimental and theoretical studies.^{6–13} Furthermore, these CT-active states are nonequilibrium states, and their formation is conformationally gated.^{13–16}

DNA CT can also be observed by measuring the chemical decomposition yields of the bases themselves, with guanine being the most reactive to oxidative damage.¹⁷ Guanine degradation after oxidation is measured by strand cleavage at damage sites, or by direct measurement of decomposition products. Because guanine radical decomposition is slow (milliseconds) in the absence of additional reactive species, such as superoxide,¹⁸ this measure of hole arrival is convoluted with the trapping and back electron transfer rates.^{19,20} We have recently studied CT yield using fast N-cyclopropyl radical traps²¹ as substituents on guanine (CPG),^{16,20} adenine (CPA),²² and cytosine (CPC)⁸ through the exocyclic amines. The subnanosecond decomposition of these

traps upon oxidation or reduction allows measurement of pre-equilibrium hole occupation.²⁰ Notably, oxidation of CPG by a tethered, photoexcited rhodium intercalator has the same periodicity with respect to adenine tract length as does the CT quenching of photoexcited Ap by guanine.¹⁶ Although the ring-opening rates have not been directly measured, there is ample evidence supporting picosecond ring-opening, including competition²⁰ with the subpicosecond recombination²³ between CPG radical cation and thionine radical anion, and competition²⁴ with picosecond recombination²⁵ ($>5 \times 10^{-9} \text{ s}^{-1}$) between CPG radical cation and aminopurine radical anion. It is also noteworthy that fluorescence spectra for duplexes containing ApA^{CPG} versus those containing ApAG are identical.²⁴

Here, we measure the quantum yields of total CT in comparable assemblies containing Ap and CPG separated by adenine tracts. Single-step CT yield is obtained from previous measurements of steady-state fluorescence quenching in the same sequences.⁵ In these fluorescence experiments, the differences in Ap emission between sequences with inosine, where there is no CT, and sequences with guanine are compared; the amount of relative quenching from photoexcited Ap reports on the single-step CT to the distant base. This depopulation, detected from the donor, but reliant on the nature of the acceptor, even several base positions away, can only be due to single-step CT between the donor and the acceptor. In multistep charge transfer to guanine, the initial depopulation of excited aminopurine occurs by oxidation of the bridge. Because substitution of inosine for guanine should not affect this initial step, the inosine-containing duplexes serve as a control for this Ap* relaxation mechanism.

Received: August 5, 2010

Published: February 24, 2011

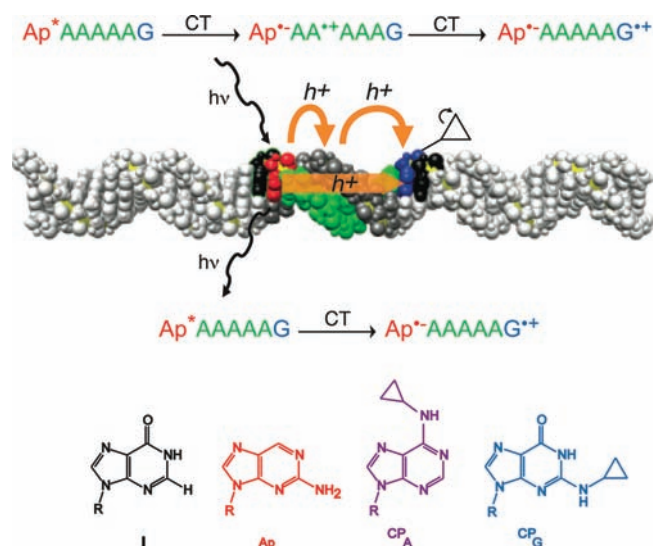


Figure 1. Pathways for single-step and multistep CT. 2-Aminopurine (Ap) is selectively excited and relaxes to an excited state that is competent for oxidizing guanine (blue; bottom reaction) through the adenine bridge in a coherent single-step process or oxidizing adenine(s) (green) as an intermediate step(s). A hole on adenine can then hop to the guanine, resulting in multistep CT (top reaction). These CT processes are in competition with emission; hence, emission yield is attenuated by CT. Structures of the four unnatural bases employed are also shown. The DNA image was constructed using coordinates generated with the model.it Server.⁴⁵

By comparing single-step and total charge transport yields, we delineate single-step and multistep contributions to DNA-mediated charge transport for a series of guanine-terminated adenine tracts (Figure 1). We establish that for some long DNA assemblies, DNA CT is a single-step process. These results underscore the importance of long-range, coherent steps in DNA-mediated charge transport across delocalized domains,⁵ and the inadequacy of hopping between localized sites as the sole mechanism for long-range CT through DNA.⁴

EXPERIMENTAL SECTION

Oligonucleotide Synthesis. DNA oligonucleotides were synthesized trityl-on using standard phosphoramidite chemistry on an ABI DNA synthesizer with Glen Research reagents. 2-Aminopurine (Ap) was incorporated as the N_2 -dimethylaminomethylidene protected phosphoramidite (Glen Research). CP_G -modified oligonucleotides were prepared by incorporating the precursor base, 2-fluoro- O_6 -paraphenylethyl-2'-deoxyinosine (Glen Research), as a phosphoramidite at the desired position.¹⁵ The resin was then reacted with 1 M diaza-(1,3)bicyclo[5.4.0]undecane (DBU, Aldrich) in acetonitrile to effectively remove the O_6 protecting group. Similarly, CP_A -modified oligonucleotides were prepared by incorporating the precursor base, O_6 -phenyl-2'-deoxyinosine (Glen Research), as a phosphoramidite at the desired position.²² For both CP_G - and CP_A -containing strands, the oligonucleotides were subsequently incubated overnight in 6 M aqueous cyclopropylamine (Aldrich) at 60 °C, resulting in substitution, base deprotection, and simultaneous cleavage from the resin. The cleaved strands were dried in vacuo and purified by reversed-phase HPLC, detritylated by 80% acetic acid for 15 min, and repurified by reversed-phase HPLC. Oligonucleotides were characterized by MALDI-TOF mass spectrometry. Sequences are provided in Table S1.

All oligonucleotides were suspended in a buffer containing 50 mM NaCl, 5 mM sodium phosphate, pH 7, and quantified using UV-visible spectroscopy. Duplexes were prepared by heating equal concentrations of complementary strands to 90 °C for 5 min and slow cooling to ambient temperature.

Photooxidation Experiments. Samples were irradiated at ambient temperature. Duplexes (30 μ L, 10 μ M) in PBS were irradiated on a 1000 W Hg/Xe lamp equipped with a monochromator at 325 nm for 30 s unless otherwise indicated. To analyze for CP_A or CP_G decomposition following irradiation, samples were digested to the component nucleosides by phosphodiesterase I (USB) and alkaline phosphatase (Roche) to completion. The resulting deoxynucleosides were analyzed by reversed-phase HPLC using a Chemcobond 5-ODS-H, 4.6 mm \times 100 mm column. The amount of CP_G or CP_A per duplex was determined by taking the ratio of the area of the HPLC peak for d^{CP_G} or d^{CP_A} to the area of the peak for dT, the internal reference. The decomposition yield is taken as the percent loss of CP_G or CP_A between an irradiated sample and the dark control; at least nine samples and three dark controls are performed for each sequence. Dark control HPLC traces were quantified for the relative amounts of dA, dC, dG, dI, dT, d^{CP_A} , and d^{CP_G} based on duplex sequence, to confirm strand stoichiometry. Actinometry was performed using a 6 mM ferrioxalate standard.²⁶ The given quantum yield is for the efficiency of formation of the ring-opened product per photon absorbed by 2-aminopurine. Errors are presented at 90% standard error of the mean (sem), using the Student's *t*-distribution at the appropriate degrees of freedom to determine confidence intervals, and each point represents at least nine replicates.

RESULTS AND DISCUSSION

Duplex Assemblies. To determine the total quantum yield of guanine oxidation by photoexcited Ap, we constructed a series of duplex assemblies with Ap separated from CP_G by adenine tracts of varying length and measured the decomposition of the radical trap upon irradiation. By comparing the yields of total and single-step CT, we determine the relative contributions of single- and multistep channels (Figure 1). Because CP_G is a fast radical trap, its decomposition yield represents the total yield of all pathways that lead to oxidation of guanine, as long as back electron transfer is slower than ring-opening. For direct comparison of guanine and adenine oxidation, we also constructed assemblies containing the CP_A radical trap at various positions along the bridge. We use $Ap-A_n-CP_A-A_m-Y$ to indicate a sequence with an adenine tract of length $n + m + 1$, with CP_A at the $n + 1$ position, and terminal base Y at the end of the tract (Y = G, I, or CP_G). All eight nucleosides are well resolved by HPLC, allowing straightforward quantification of the CP_G or CP_A content per duplex, and the inosine barriers isolate charge transfer from occurring between the ApA_nY containing region and the rest of the construct.^{15,27}

Quantum Yields for CT. The routes for fluorescence quenching of photoexcited Ap in oligonucleotides have been characterized in detail. The fluorescence of photoexcited Ap in DNA is quenched versus the free nucleoside, even if there is no guanine in the assembly. The presence of a nearby guanine leads to additional quenching of fluorescence by a CT mechanism.^{3,5,24,25,27–29} Adenine oxidation by photoexcited Ap, while favorable, is far slower than guanine oxidation, as is reduction of cytosine and thymidine by photoexcited Ap.²⁵ Recent time-resolved fluorescence and transient absorption measurements have revealed that there is a short-lived (≤ 200 fs) excited state of aminopurine that primarily decays through a dark state, with a

fraction undergoing relaxation to the longer-lived emissive state capable of CT.³⁰

On the basis of the known photophysics of aminopurine in DNA, a limit can be inferred for the quantum yield of single-step CT based on the quantum yields of emission from a duplex with a CT-accessible guanine and the analogous duplex replacing guanine with the redox-inactive nucleotide inosine. The relaxation pathways available to an inosine-containing assembly are described in panel A in Figure S1. It is apparent that

$$\Phi_{\text{em}}^{\text{I}} = (1 - \Phi_{\text{nr-d}})\Phi_{\text{rel} \rightarrow \text{em}}^{\text{I}} = (1 - \Phi_{\text{nr-d}})\frac{k_{\text{em}}}{k_{\text{em}} + k_{\text{A}}}$$

where $\Phi_{\text{em}}^{\text{I}}$ is the quantum yield of emission from an inosine-containing duplex, $\Phi_{\text{nr-d}}$ is the quantum yield of hot deactivation through a dark state,³⁰ $\Phi_{\text{rel} \rightarrow \text{em}}^{\text{I}}$ is the efficiency of emission from the emissive state of aminopurine, k_{em} is the rate of emission from this state, and k_{A} is the rate of charge transfer to adenine from the emissive state of aminopurine.

For a guanine-containing assembly,

$$\Phi_{\text{em}}^{\text{G}} = (1 - \Phi_{\text{nr-d}})\Phi_{\text{rel} \rightarrow \text{em}}^{\text{G}} = (1 - \Phi_{\text{nr-d}})\frac{k_{\text{em}}}{k_{\text{em}} + k_{\text{A}} + k_{\text{G}}}$$

where k_{G} is the rate of charge transfer from the emissive state of aminopurine to guanine across the adenine tract. The quantum yield of CT to guanine is

$$\Phi_{\text{CT}}^{\text{G}} = (1 - \Phi_{\text{nr-d}})\frac{k_{\text{G}}}{k_{\text{em}} + k_{\text{A}} + k_{\text{G}}} = (1 - \Phi_{\text{nr-d}})\left(1 - \frac{\Phi_{\text{em}}^{\text{G}}}{\Phi_{\text{em}}^{\text{I}}}\right)$$

A lower limit can be set on $\Phi_{\text{CT}}^{\text{G}}$ because

$$\Phi_{\text{em}}^{\text{I}} \leq (1 - \Phi_{\text{nr-d}})$$

and hence

$$\Phi_{\text{CT}}^{\text{G}} = (1 - \Phi_{\text{nr-d}})\left(1 - \frac{\Phi_{\text{em}}^{\text{G}}}{\Phi_{\text{em}}^{\text{I}}}\right) \geq \Phi_{\text{em}}^{\text{I}} - \Phi_{\text{em}}^{\text{G}}$$

This result is intuitive, as the difference between the quantum yields of emission in the presence and absence of guanine is due to single-step CT from aminopurine to guanine.

We therefore compare in Figure 2 the values obtained as lower limits for single-step CT measured by fluorescence quenching (red) to our measurements for total CT yield from $^{\text{CPG}}$ decomposition (blue). Upon irradiation, decomposition is observed for $^{\text{CPG}}$, indicating oxidation of guanine by photoexcited Ap (Table S2). For short donor–acceptor separation ($n = 0–2$), little ring-opening occurs, because charge recombination between the aminopurine anion radical and guanine cation radical is competitive with radical trapping at the $^{\text{CPG}}$ (Figure 2).^{16,24} However, with four intervening adenines, $^{\text{CPG}}$ radical decomposition outcompetes charge recombination. The quantum yield for ring-opening with respect to generation of excited Ap peaks at about 1% with four intervening adenines followed by a slow decay with longer sequences. The profile for $^{\text{CPG}}$ decomposition as a function of distance is similar to that which has previously been observed in other assemblies for oxidation of $^{\text{CPG}}$ by photoexcited Ap.¹⁶ Interestingly, the peak value is comparable to the quantum yield (1.7%) of emission from Ap–(A)_{*n*}–I sequences,⁵ which reflects the maximum yield of CT that can be achieved.

For longer A-tracts, with 4–6 intervening adenines, where charge recombination is not competitive, we see that the quantum yield for single-step CT, obtained through fluorescence

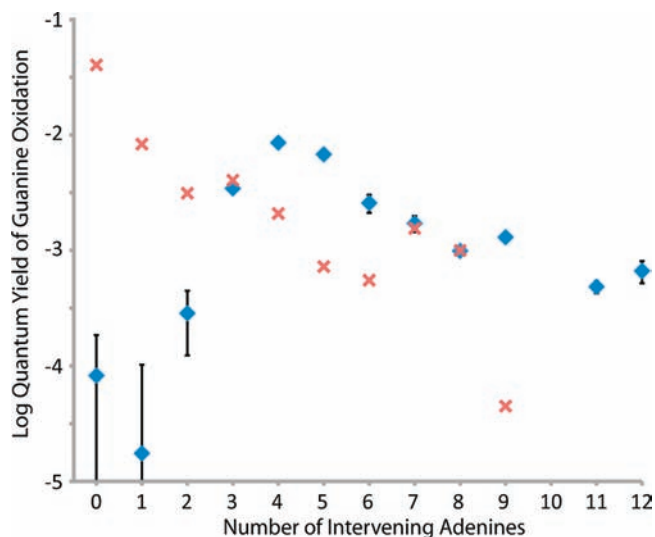


Figure 2. Semilog plot of CT quantum yields as a function of bridge length for the Ap–A_{*n*}–^{CPG}G series (blue ♦), as determined by ring-opening of ^{CPG}G. The experiments were repeated at least nine times, the results averaged, and the error is expressed as 90% sem. Error bars that are not shown are smaller than the data point. On the same plot, single-step CT yields for the analogous duplexes are shown for comparison (red ×'s, data from ref 5).

quenching, does not account for the total CT quantum yield, obtained through $^{\text{CPG}}$ decomposition (Figure 2). Photoexcited Ap is competent to oxidize adenine directly, generating a hole that can rapidly migrate across the adenine tract to guanine,^{4,31} and thus some component of multistep CT is to be expected. Unexpectedly, however, with 7 or 8 intervening adenines, the quantum yields for single-step CT and total CT are equal; CT appears to be coherent for $n = 7, 8$. As detailed above, the yields of single-step CT determined from fluorescence quenching and presented in Figure 2 are lower limits on the actual yield of single-step CT. If CT to guanine competes with CT to adenine, or with conversion to other nonemissive states, then the true yield of single-step CT must be higher than the values we use for the analysis here. On the other hand, in the absence of back electron transfer, total CT is necessarily greater than or equal to the single-step component. To summarize:

$$\Phi_{\text{em}}^{\text{I}} - \Phi_{\text{em}}^{\text{G}} \leq \Phi_{\text{CT}}^{\text{G}} \leq \Phi_{\text{CT}, \text{total}}^{\text{G}} \leq \Phi_{\text{CT}, \text{total}}^{\text{CPG}}$$

That $\Phi_{\text{em}}^{\text{I}} - \Phi_{\text{em}}^{\text{G}}$ is the same as $\Phi_{\text{CT}, \text{total}}^{\text{CPG}}$ for $n = 7, 8$ implies that $\Phi_{\text{CT}}^{\text{G}} = \Phi_{\text{CT}, \text{total}}^{\text{G}}$ for these bridges and further validates the model for the excited-state dynamics that we have assumed.

Coherent CT across Domains. It is noteworthy that CT appears to be in a single step in those assemblies where the periodic variation in fluorescence quenching is a maximum. We have proposed that these periodicities in CT depend upon transient delocalized domains in the DNA duplex, and how well an assembly can structurally and dynamically accommodate such a domain. From the data presented here, it appears that when the domain is well accommodated, CT is coherent.^{5,32} Moreover, that coherence arises in the domain, including Ap, the 7–8 intervening adenines, and guanine, representing essentially a full turn of the DNA helix (Figure 3).

An important consideration, in this context, is whether delocalization itself could slow the ring-opening rate of the $^{\text{CPG}}$. Both experimental and theoretical studies have clearly

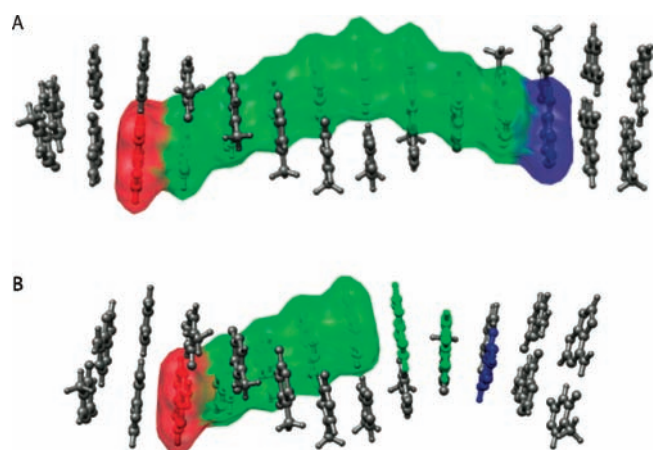


Figure 3. The higher yield of single-step CT through the eight-adenine tract versus the six-adenine tract is a property of the sequence of the DNA, rather than the distance between the donor and the acceptor. An integer number of fully delocalized domains can be accommodated along the eight-adenine tract, allowing CT between the donor and acceptor and delocalization across the full helical turn (A). The six-adenine tract, below, cannot accommodate delocalized domains along its entire length (B), and single-step CT is limited to a less ideal bridging structure. The DNA image was constructed using coordinates generated with the model.it Server.⁴⁵

supported delocalized, CT-active states to be nonequilibrium and populated on the picosecond time-scale,^{13–15,33} with rapid localization of the hole onto a single nucleotide.^{6d,34} Localization of the guanine radical cation occurs on a time-scale similar to that of ring-opening, and certainly far faster than recombination, indicating that the hole trapping rate should be unaffected by domains.

Transition to Single-Step CT. Furthermore, these data provide the first case of single-step CT overtaking incoherent CT at longer distances. This transition is opposite to that generally observed in molecular bridges.^{35–38} The changing contributions of the two mechanisms could not have been determined by solely measuring the total CT yield as a function of distance. The distance dependence for $n > 4$ is fit comparably by a geometric or an exponential decay (Figure S2); generally, fits of CT rates to these two decays tend to be equivalent for moderate bridge lengths.³⁹ In fact, the distance dependence of the total yield is similar to that observed for total CT between stilbenes in photoexcited stilbene-capped DNA hairpins, despite that system being incompetent for coherent CT over more than two base pairs.⁴⁰ The geometric dependence gives an η of 2.6, corresponding to a small bias toward migration away from the ^{CP}G,⁴¹ probably due to Coulombic attraction to the aminopurine anion radical.⁴²

Oxidation of the Adenine Bridge. To measure oxidation of the bridge, we inserted ^{CP}A, an unnatural adenine analogue, into the adenine tract. The potential of the Ap excited state is barely adequate for adenine oxidation,²⁵ but we find rapid decomposition of ^{CP}A upon irradiation of Ap-containing duplexes (Figure S3).⁴³ As ^{CP}A is moved along the 5-adenine tract, there is the same initial increase in yield due to charge recombination competing less favorably with trapping (Table S2). We would expect that ^{CP}A in the adenine tract would interfere with multistep hopping of a hole to ^{CP}G. Accordingly, far less ^{CP}G decomposition is observed for Ap–A₂–^{CP}A–A₂–^{CP}G and Ap–A₂–^{CP}A–A₃–^{CP}G than the respective assemblies without

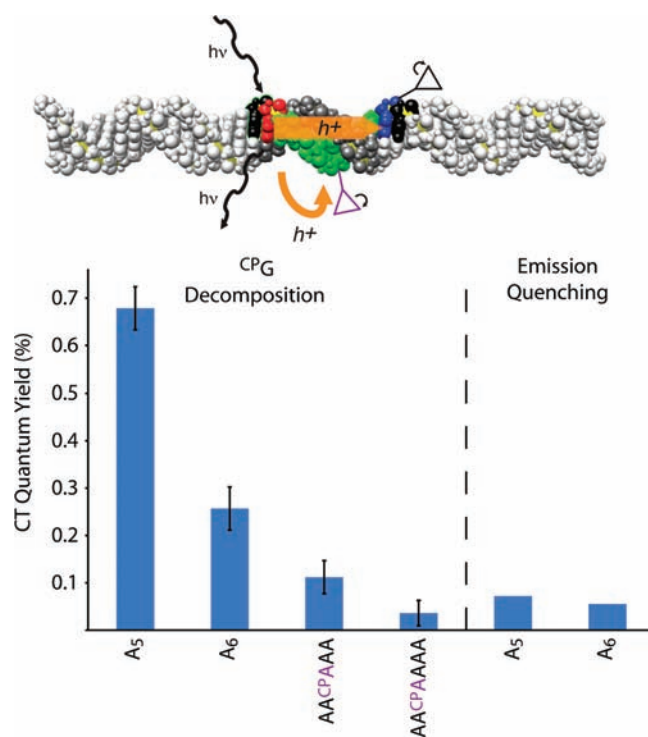


Figure 4. A ^{CP}A inside the adenine tract disrupts multistep CT to ^{CP}G by intercepting the hole. CT through the sequences Ap–A₅–^{CP}G and Ap–A₆–^{CP}G is mostly multistep, and the intervening ^{CP}A disrupts CT substantially, but not totally. The remaining CT yield when multistep transport is blocked is the same as the single-step CT yield determined for these sequences from fluorescence quenching, validating our complementary measurements of the two channels. Error bars are 90% sem. The DNA image was constructed using coordinates generated with the model.it Server.⁴⁵

^{CP}A, Ap–A₅–^{CP}G, and Ap–A₆–^{CP}G (Figure 4). For both bridge lengths, the quantum yield of ^{CP}G decomposition when multistep transport is blocked is similar to the quantum yield of emission quenching by guanine. These results provide further support to our assignment of the yield of emission quenching as the yield of single-step CT to guanine.

We also see evidence for delocalization from the sensitivity of ^{CP}A decomposition to the sequence distal to the photooxidant. Significantly less ^{CP}A decomposition is observed for Ap–A₂–^{CP}A–A₂–^{CP}G than for Ap–A₂–^{CP}A–A₃–^{CP}G, where the only difference is the number of adenines between ^{CP}A and ^{CP}G (Table S2). For two, but not three intervening adenines, ^{CP}G is competent to compete with ^{CP}A for the radical. This sensitivity to a distal trap could be due to either polaron formation^{6,7,19} or transient delocalization along the adenine tract and ^{CP}G reporter. We have previously observed similar behavior for oxidation of the higher potential ^{CP}C near ^{CP}G, although in that case competition was not apparent for more than a single intervening adenine.⁸ Furthermore, Ap–A₃–^{CP}A–A–I and Ap–A₃–^{CP}A–A₄–I differ only in the length of the adenine tract, yet the quantum yield of ^{CP}A decomposition increases by 50% for the latter assembly. The longer adenine tract has more runs of AT base pairs that include the ^{CP}A, and hence can accommodate more low-potential delocalized orbitals. Again, both a self-trapped polaron following injection and transient delocalization prior to injection are consistent with this interpretation.

Intriguingly, $^{\text{CP}}$ A decomposition is insensitive to whether the distant base is inosine or guanine. When there is no guanine at the end of the adenine tract, the single-step CT pathway that leads to fluorescence quenching is eliminated. If single- and multistep CT are in competition, eliminating single-step CT to guanine should lead to an increase in the yield of $^{\text{CP}}$ A oxidation, but such an increase is not observed. Hence, single- and multistep CT must be proceeding from different populations. This is consistent with the temperature dependence of the emissive Ap picosecond decay components, which supports the presence of two different populations of assemblies; those in an initially CT-active state proceed to rapid CT, while CT for those in a less active configuration is conformationally gated.¹⁴

CONCLUSIONS

Over a long adenine tract that can accommodate well-stacked, delocalized domains, long-distance, single-step CT dominates the overall transport from aminopurine to guanine. At other separations, multistep CT is dominant, even in sequences with shorter donor–acceptor separation, where dynamic delocalized domains do not span the construct. These results reflect the exquisite sensitivity to base stacking that has been documented and underscore the importance of sequence-dependent conformational dynamics in the mechanism and yields of DNA-mediated CT. CT through DNA can occur effectively through transiently delocalized regions of the duplex, indeed through a fully delocalized helical turn of DNA. Significantly, models of charge migration in DNA must consider the contribution of coherent transfer over long distances.

ASSOCIATED CONTENT

S Supporting Information. Figures S1–S3 and Tables S1 and S2, including complete sequences and $^{\text{CP}}$ G decomposition quantum yields. This material is available free of charge via the Internet at <http://pubs.acs.org>.

AUTHOR INFORMATION

Corresponding Author
jkbarton@caltech.edu

ACKNOWLEDGMENT

We are grateful to the National Institutes of Health (GM49216) for their support. We also thank the Caltech SURF program for a summer undergraduate fellowship (S.M.W.).

REFERENCES

- (1) (a) Gorodetsky, A. A.; Buzzeo, M. C.; Barton, J. K. *Bioconjugate Chem.* **2008**, *19*, 2285–2296. (b) Genereux, J. C.; Boal, A. K.; Barton, J. K. *J. Am. Chem. Soc.* **2010**, *132*, 891–905. (c) Guo, X.; Gorodetsky, A. A.; Hone, J.; Barton, J. K.; Nuckolls, C. *Nat. Nanotechnol.* **2008**, *3*, 163–167.
- (2) (a) Genereux, J. C.; Barton, J. K. *Chem. Rev.* **2009**, *110*, 1642–1662. (b) Mallajosyula, S. S.; Pati, S. K. *J. Phys. Chem. Lett.* **2010**, *1*, 1881–1894. (c) Wagenknecht, H.-A. *Charge Transfer in DNA: From Mechanism to Application*; Wiley VCH: Weinheim, Germany, 2005. (d) Wagenknecht, H.-A. *Nat. Prod. Rep.* **2006**, *23*, 973–1006.
- (3) Kelley, S. O.; Barton, J. K. *Science* **1999**, *283*, 375–381.
- (4) Nuñez, M. E.; Hall, D. B.; Barton, J. K. *Chem. Biol.* **1999**, *6*, 85–97.

- (5) O'Neill, M. A.; Barton, J. K. *J. Am. Chem. Soc.* **2004**, *126*, 11471–11483.
- (6) (a) Schuster, G. B. *Acc. Chem. Res.* **2000**, *33*, 253–260. (b) Barnett, R. N.; Cleveland, C. L.; Joy, A.; Landman, U.; Schuster, G. B. *Science* **2001**, *294*, 567–571. (c) Zeidan, T. A.; Carmieli, R.; Kelley, R. F.; Wilson, T. M.; Lewis, F. D.; Wasielewski, M. R. *J. Am. Chem. Soc.* **2008**, *130*, 13945–13955. (d) Kucherov, V. M.; Kinz-Thompson, C. D.; Conwell, E. M. *J. Phys. Chem. C* **2010**, *114*, 1663–1666.
- (7) (a) Basko, D. M.; Conwell, E. M. *Phys. Rev. Lett.* **2002**, *88*, 098102. (b) Conwell, E. M.; Bloch, S. M.; McLaughlin, P. M.; Basko, D. M. *J. Am. Chem. Soc.* **2007**, *129*, 9175–9181.
- (8) (a) Shao, F.; Augustyn, K. E.; Barton, J. K. *J. Am. Chem. Soc.* **2005**, *127*, 17445–17452. (b) Shao, F.; O'Neill, M. A.; Barton, J. K. *Proc. Natl. Acad. Sci. U.S.A.* **2004**, *101*, 17914–17919.
- (9) (a) Adhikary, A.; Kumar, A.; Khanduri, D.; Sevilla, M. D. *J. Am. Chem. Soc.* **2008**, *130*, 10282–10292. (b) Kobayashi, K. *J. Phys. Chem. B* **2010**, *114*, 5600–5604.
- (10) (a) Renger, T.; Marcus, R. A. *J. Phys. Chem. A* **2004**, *107*, 8404–8419. (b) Jakobsson, M.; Stafström, S. *J. Chem. Phys.* **2008**, *129*, 125102.
- (11) (a) Buchvarov, I.; Wang, Q.; Raytchev, M.; Trifonov, A.; Fiebig, T. *Proc. Natl. Acad. Sci. U.S.A.* **2007**, *104*, 4794–4797. (b) Conwell, E. M. *J. Phys. Chem. B* **2008**, *112*, 2268–2272.
- (12) (a) Lewis, J. P.; Cheatham, T. E., III; Starikov, E. B.; Wang, H.; Sankey, O. F. *J. Phys. Chem. B* **2003**, *107*, 2581–2587. (b) Hatcher, E.; Balaeff, A.; Keinan, S.; Venkatramani, R.; Beratan, D. N. *J. Am. Chem. Soc.* **2008**, *130*, 11752–11761. (c) Bongiorno, A. *J. Phys. Chem. B* **2008**, *112*, 13945–13950. (d) Kubar, T.; Kleinekathofer, U.; Elstner, M. *J. Phys. Chem. B* **2009**, *113*, 13107–13117.
- (13) O'Neill, M. A.; Barton, J. K. *J. Am. Chem. Soc.* **2004**, *126*, 13234–13235.
- (14) O'Neill, M. A.; Becker, H.-C.; Wan, C.; Barton, J. K.; Zewail, A. H. *Angew. Chem., Int. Ed.* **2003**, *42*, 5896–5900.
- (15) (a) Troisi, A.; Orlandi, G. *J. Phys. Chem. B* **2002**, *106*, 2093–2101. (b) Reha, D.; Barford, W.; Harris, S. *Phys. Chem. Chem. Phys.* **2008**, *10*, 5436–5444. (c) Steinbrecher, T.; Koslowski, T.; Case, D. A. *J. Phys. Chem. B* **2008**, *112*, 16935–16944.
- (16) Genereux, J. C.; Augustyn, K. E.; Davis, M. L.; Shao, F.; Barton, J. K. *J. Am. Chem. Soc.* **2008**, *130*, 15150–15156.
- (17) (a) Hall, D. B.; Holmlin, R. E.; Barton, J. K. *Nature* **1996**, *382*, 731–735. (b) Senthilkumar, K.; Grozema, F. C.; Guerra, C. F.; Bickelhaupt, F. M.; Lewis, F. D.; Berlin, Y. A.; Ratner, M. A.; Siebbeles, L. D. A. *J. Am. Chem. Soc.* **2005**, *127*, 14894–14903. (c) Kanvah, S.; Joseph, J.; Schuster, G. B.; Barnett, R. N.; Cleveland, C. L.; Landman, U. *Acc. Chem. Res.* **2009**, *43*, 280–287.
- (18) (a) Misiaszek, R.; Crean, C.; Joffe, A.; Geacintov, N. E.; Shafirovich, V. *J. Biol. Chem.* **2004**, *279*, 32106–32115. (b) Stemp, E. D. A.; Arkin, M. R.; Barton, J. K. *J. Am. Chem. Soc.* **1997**, *119*, 2921–2925.
- (19) Liu, C.-S.; Hernandez, R.; Schuster, G. B. *J. Am. Chem. Soc.* **2004**, *126*, 2877–2884.
- (20) Williams, T. T.; Dohno, C.; Stemp, E. D. A.; Barton, J. K. *J. Am. Chem. Soc.* **2004**, *126*, 8148–8158.
- (21) (a) Nakatani, K.; Dohno, C.; Saito, I. *J. Am. Chem. Soc.* **2001**, *123*, 9681–9682. (b) Dohno, C.; Ogawa, A.; Nakatani, K.; Saito, I. *J. Am. Chem. Soc.* **2003**, *125*, 10154–10155.
- (22) Augustyn, K. E.; Genereux, J. C.; Barton, J. K. *Angew. Chem., Int. Ed.* **2007**, *46*, 5731–5733.
- (23) (a) Dohno, C.; Stemp, E. D. A.; Barton, J. K. *J. Am. Chem. Soc.* **2003**, *125*, 9586–9587. (b) Reid, G. D.; Whittaker, D. J.; Day, M. A.; Turton, D. A.; Kayser, V.; Kelly, J. M.; Beddard, G. S. *J. Am. Chem. Soc.* **2002**, *124*, 5518–5527.
- (24) O'Neill, M. A.; Dohno, C.; Barton, J. K. *J. Am. Chem. Soc.* **2004**, *126*, 1316–1317.
- (25) Wan, C.; Fiebig, T.; Schiemann, O.; Barton, J. K.; Zewail, A. H. *Proc. Natl. Acad. Sci. U.S.A.* **2000**, *97*, 14052–14055.
- (26) Hatchard, C. G.; Parker, C. A. *Proc. R. Soc. London, Ser. A* **1956**, *235*, 518.

- (27) O'Neill, M. A.; Barton, J. K. *Proc. Natl. Acad. Sci. U.S.A.* **2002**, *99*, 16543–16550.
- (28) Somsen, O. J. G.; Keukens, L. B.; de Keijzer, M. N.; van Hoek, A.; van Amerongen, H. *ChemPhysChem* **2005**, *6*, 1622–1627.
- (29) Manoj, P.; Min, C.-K.; Aravindakumar, C. T.; Joo, T. *Chem. Phys.* **2008**, *352*, 333–338.
- (30) Wan, C.; Xia, T.; Becker, H.-C.; Zewail, A. H. *Chem. Phys. Lett.* **2005**, *412*, 158–163.
- (31) Takada, T.; Kawai, K.; Cai, X.; Sugimoto, A.; Fujitsuka, M.; Majima, T. *J. Am. Chem. Soc.* **2004**, *126*, 1125–1129.
- (32) Valis, L.; Wang, Q.; Raytchev, M.; Buchvarov, I.; Wagenknecht, H.-A.; Fiebig, T. *Proc. Natl. Acad. Sci. U.S.A.* **2006**, *103*, 10192–10195.
- (33) Adhikary, A.; Khanduri, D.; Sevilla, M. D. *J. Am. Chem. Soc.* **2009**, *131*, 8614–8619.
- (34) (a) Voityuk, A. A. *J. Chem. Phys.* **2005**, *122*, 204904. (b) Kinz-Thompson, C.; Conwell, E. *J. Phys. Chem. Lett.* **2010**, *1*, 1403–1407. (c) Kurnikov, I. V.; Tong, G. S. M.; Madrid, M.; Beratan, D. N. *J. Phys. Chem. B* **2002**, *106*, 7. (d) Uskov, D. B.; Burin, A. L. *Phys. Rev. B* **2008**, *78*, 073106.
- (35) (a) Weiss, E. A.; Ratner, M. A.; Wasielewski, M. R. *Top. Curr. Chem.* **2005**, *257*, 103–133. (b) Davis, W. B.; Svec, W. A.; Ratner, M. A.; Wasielewski, M. R. *Nature* **1998**, *396*, 60–63.
- (36) (a) Choi, S. H.; Kim, B. S.; Frisbie, C. D. *Science* **2008**, *320*, 1482–1486. (b) Choi, S. H.; Risko, C.; Ruiz Delgado, M. C.; Kim, B. S.; Brédas, J.-L.; Frisbie, C. D. *J. Am. Chem. Soc.* **2010**, *132*, 4358–4368. (c) Luo, L.; Frisbie, C. D. *J. Am. Chem. Soc.* **2010**, *132*, 8854–8855.
- (37) (a) Paul, A.; Watson, R. M.; Lund, P.; Xing, Y.; Burke, K.; He, Y.; Borguet, E.; Achim, C.; Waldeck, D. H. *J. Phys. Chem. C* **2008**, *112*, 7233–7240. (b) Paul, A.; Watson, R. M.; Wierzbinski, E.; Davis, K. L.; Sha, A.; Achim, C.; Waldeck, D. M. *J. Phys. Chem. B* **2010**, *114*, 14140–14148.
- (38) Giese, B.; Amaudrut, J.; Köhler, A.-K.; Spormann, M.; Wessely, S. *Nature* **2001**, *412*, 318–320.
- (39) Goldsmith, R. H.; DeLeon, O.; Wilson, T. M.; Finkelstein-Shapiro, D.; Ratner, M. A.; Wasielewski, M. R. *J. Phys. Chem. A* **2008**, *112*, 4410–4414.
- (40) Lewis, F. D.; Zhu, H.; Daublain, P.; Cohen, B.; Wasielewski, M. R. *Angew. Chem., Int. Ed.* **2006**, *45*, 7982–7995.
- (41) Jortner, J.; Bixon, M.; Langenbacher, T.; Michel-Beyerle, M. E. *Proc. Natl. Acad. Sci. U.S.A.* **1998**, *95*, 12759–12765.
- (42) Grozema, F. C.; Tonzani, S.; Berlin, Y. A.; Schatz, G. C.; Siebbeles, L. D. A.; Ratner, M. A. *J. Am. Chem. Soc.* **2008**, *130*, 5157–5166.
- (43) The potentials of A and ^{CP}A have not been experimentally compared, and neither has been measured as a DNA-incorporated species. Electrochemical studies on free nucleosides^{21b,44} suggest that the oxidation potential of ^{CP}A might be as much as 200 mV below that of A. While we are skeptical regarding the relevance of aqueous nucleotide potentials to hole potentials in DNA, it is possible that ^{CP}A is more effective than A at intercepting the hole based on a lower potential.
- (44) Okamoto, A.; Tanaka, K.; Saito, I. *J. Am. Chem. Soc.* **2003**, *125*, 5066–5071.
- (45) Munteanu, M. G.; Vlahovicek, K.; Parthasaraty, S.; Simon, I.; Pongor, S. *Trends Biochem. Sci.* **1998**, *23*, 341–346.